

# The Corrected Inverse-Gaussian: A Tractable First-Hitting-Time Channel Model for Nonstationary Molecular Communication

Yen-Chi Lee

Department of Mathematics  
National Central University, Taiwan  
Email: ycllee@math.ncu.edu.tw

**Abstract**—This paper develops a tractable analytical channel model for first-hitting-time molecular communication (MC) systems under time-varying drift. While existing studies of nonstationary transport rely primarily on numerical solutions of advection–diffusion equations or parametric impulse-response fitting, they do not provide an explicit analytical description of trajectory-level arrival dynamics at absorbing boundaries. By adopting a change-of-measure formulation, we reveal a structural decomposition of the first-hitting-time density into a cumulative-drift displacement term and a stochastic boundary-flux modulation factor. This leads to a closed-form Corrected-Inverse-Gaussian (C-IG) density that generalizes the classical IG model to nonstationary drift while preserving  $O(1)$  evaluation complexity. Monte Carlo simulations under both smooth pulsatile and abrupt switching drift profiles confirm that the proposed C-IG model accurately captures complex transport phenomena, including phase modulation, multi-pulse dispersion, and transient backflow—effects that traditionally complicate symbol synchronization and induce severe inter-symbol interference. The resulting framework provides a physics-informed, computationally efficient channel model suitable for system-level analysis and advanced receiver design, such as real-time maximum likelihood detection, in dynamic biological and MC environments.

**Index Terms**—Molecular communications, channel modeling, time-varying drift, nonstationary channels, first-hitting-time.

## I. INTRODUCTION

Diffusion-based molecular communication (MC) channels are governed by the stochastic transport of signaling molecules through diffusion and advection [1], [2]. The dominant modeling paradigm characterizes such channels via concentration-based impulse responses [3] derived from advection–diffusion partial differential equations (PDEs) [4]. Under steady and uniform drift conditions, these formulations admit compact analytical expressions [1]. For absorbing receiver settings, the first-hitting-time (FHT) distribution provides a natural description of molecule arrival dynamics. In particular, when drift is constant, the FHT density follows the classical Inverse-Gaussian (IG) distribution [5], which has been widely adopted as a tractable baseline analytical channel model in MC.

However, realistic transport conditions are rarely stationary. Pulsatile cardiovascular flows [6], [7] and time-varying electrophoretic transport in microfluidic platforms [8], [9] induce explicitly time-dependent drift velocities. Physically, these environments are commonly modeled using oscillatory

velocity profiles superimposed on a nonzero mean drift, reflecting periodically driven pressure gradients [10], [11]. This nonstationary drift reshapes arrival statistics, causing phase modulation, multi-peak behavior, and transient backflow that stationary models cannot capture.

Despite extensive studies on time-varying transport, most MC literature remains concentration-centric. While recent advances analytically model time-variant channels induced by random transceiver mobility [12], they fundamentally assume a static fluid medium. Characterizing nonstationarity from explicitly *time-varying drift* remains an open analytical challenge. Unlike mobility, which is resolvable by averaging static responses over random distances, time-varying advection continuously alters the stochastic trajectory. This triggers directional phenomena, like transient backflow, that traditional models cannot capture. Consequently, drift time-variability is typically handled via numerical advection–diffusion PDEs or simulation-calibrated impulse responses [13]. While capturing macroscopic concentration, these approaches do not yield closed-form analytical models for trajectory-level arrival statistics [14]. Stochastically, the exact time-varying FHT density can be characterized through Volterra-type integral equations [15], [16]. However, lacking closed-form solutions, these recursive formulations are unsuitable for real-time channel modeling and signal processing.

To address this, we develop a physics-informed analytical channel model for FHT behavior under *time-varying drift*. Using a change-of-measure perspective, we uncover a structural decomposition of the FHT density into a cumulative-drift displacement and a stochastic boundary-flux modulation factor. This yields a closed-form *Corrected-Inverse-Gaussian (C-IG)* density formula, extending the classical IG model to strongly nonstationary drift while preserving constant-complexity evaluation.

The main contributions of this work are summarized as follows:

- **Analytical Framework for Nonstationary Transport:** We establish a tractable analytical framework to model FHT channels under explicitly time-dependent drift velocities. By uncovering a structural decomposition of nonstationary transport into a cumulative displacement term and a stochastic boundary-flux modulation factor, this

$$\ln \frac{d\mathbb{Q}}{d\mathbb{P}} \Big|_T = \underbrace{\frac{\mu(T)\ell - \mu(0)x_0}{\sigma^2}}_{\text{Boundary Potential}} - \underbrace{\frac{1}{\sigma^2} \int_0^T \mu'(t) X_t dt}_{\text{Stochastic Coupling}} - \underbrace{\frac{1}{2\sigma^2} \int_0^T \mu(t)^2 dt}_{\text{Intrinsic Energy}}. \quad (1)$$

work extends trajectory-level channel modeling beyond the traditional stationary assumption.

- **Closed-Form Corrected-IG Density:** We derive a closed-form C-IG density that generalizes the classical IG model [5] to strongly nonstationary regimes. The resulting formulation captures complex phenomena—including phase modulation, multi-pulse dispersion, and transient backflow—while maintaining constant-time evaluation per time instance, making it suitable for real-time applications.
- **Robustness Across Diverse Drift Profiles:** Through high-precision Monte Carlo validation, we demonstrate the robustness of the C-IG model across qualitatively different scenarios, ranging from *smooth periodic* to *abrupt switching* drift. This confirms the model’s waveform-agnostic nature and establishes it as a computationally efficient alternative to PDE-based simulations for system-level analysis.

## II. STRUCTURAL DECOMPOSITION OF THE FHT DENSITY UNDER TIME-VARYING DRIFT

Exact first-passage formulations of the FHT density under time-varying drift are analytically intractable. To obtain a tractable representation, we adopt a change-of-measure framework that separates reference diffusion from drift-induced perturbations.

This formulation reveals a natural two-layer structure of the FHT density: an exponential displacement core determined by cumulative drift, and a stochastic boundary-flux modulation factor. The following subsections derive these two components.

### A. Girsanov Three-Factor Decomposition

Let  $(\Omega, \mathcal{F}, \{\mathcal{F}_t\}_{t \geq 0}, \mathbb{P})$  be a filtered probability space, and let  $W_t$  denote a standard one-dimensional Brownian motion adapted to  $\{\mathcal{F}_t\}_{t \geq 0}$  under  $\mathbb{P}$ . Under the reference measure  $\mathbb{P}$ , the signaling molecule follows drift-free diffusion,

$$dX_t = \sigma dW_t, \quad X_0 = x_0. \quad (2)$$

Under the target measure  $\mathbb{Q}$ , the dynamics incorporate a deterministic time-varying drift,

$$dX_t = \mu(t)dt + \sigma dW_t. \quad (3)$$

Assume that  $\mu(t)$  is deterministic and square-integrable on finite intervals. The stopping time to an absorbing boundary  $\ell > x_0$  is defined as  $T := \inf\{t > 0 : X_t = \ell\}$ .

By the Girsanov theorem [17], the Radon–Nikodym derivative evaluated at the stopping time  $T$  is

$$\frac{d\mathbb{Q}}{d\mathbb{P}} \Big|_T = \exp \left( \frac{1}{\sigma^2} \int_0^T \mu(t) dX_t - \frac{1}{2\sigma^2} \int_0^T \mu(t)^2 dt \right). \quad (4)$$

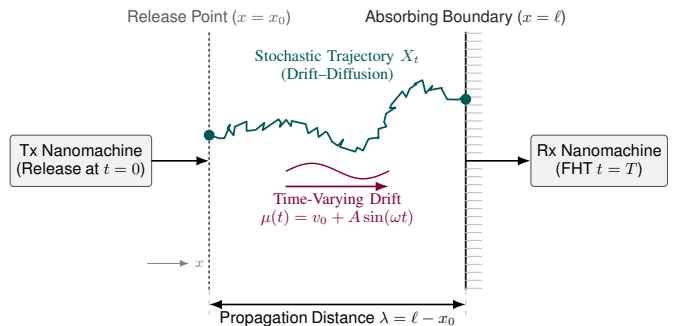


Fig. 1. Schematic illustration of the 1D molecular communication system under pulsatile flow. Information molecules are released by the Tx nanomachine at  $x_0$  and propagate through a fluid medium characterized by a constant diffusion coefficient  $\sigma^2$  and a time-varying drift velocity  $\mu(t)$ . The channel impulse response is determined by the first-hitting-time  $T$ , the random instant when the stochastic trajectory  $X_t$  first contacts the absorbing boundary at  $x = \ell$ .

Applying the Itô integration-by-parts formula (see [18]) to  $\mu(t)X_t$  and imposing the boundary conditions  $X_0 = x_0$  and  $X_T = \ell$ , the log-likelihood ratio admits a natural decomposition into three distinct components, as summarized in (1). These correspond to

- *Boundary Potential:* a term determined solely by endpoint values of the drift field,
- *Intrinsic Energy:* an accumulated deterministic cost of maintaining drift,
- *Stochastic Coupling:* a path-dependent interaction between drift variations and diffusion trajectories.

This decomposition explicitly separates geometric properties of the drift field from stochastic interference effects and provides a transparent physical interpretation of how time-varying drift modifies boundary-hitting dynamics.

### B. Extraction of the Macroscopic Exponential Core

To obtain the FHT density under time-varying drift, we evaluate the conditional expectation of the Radon–Nikodym derivative given  $T = t$ . The principal analytical difficulty arises from the *stochastic coupling* term in (1), which involves an infinite-dimensional path integral. (Note that for piecewise-smooth drift profiles, the derivation applies on each smooth segment, with discontinuities treated in a distributional sense.)

To maintain tractability, we adopt a *most-probable-path* (MPP) approximation [19] via the linear interpolation

$$\bar{X}_s \approx x_0 + \frac{s}{t}(\ell - x_0). \quad (5)$$

This choice is asymptotically justified for short-time/moderate-drift regimes and, crucially, enables a critical structural cancellation that yields a constant-complexity closed-form model.

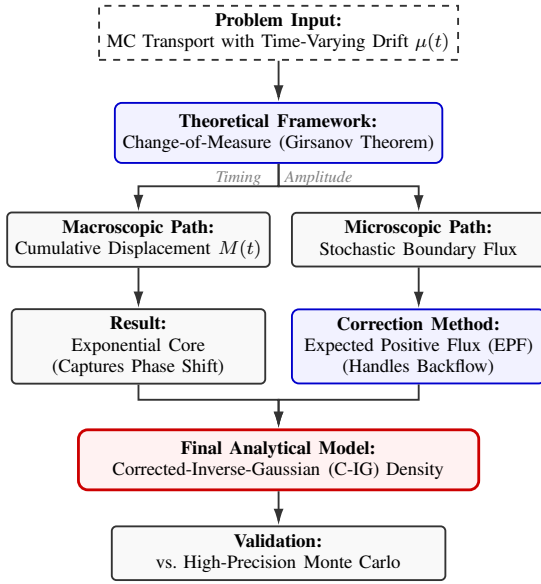


Fig. 2. Methodological flowchart of the proposed framework. The approach leverages a change-of-measure formulation to decompose nonstationary transport into deterministic cumulative displacement and stochastic flux modulation, synthesized via the EPF correction into the final closed-form C-IG model.

Substituting this MPP path into the stochastic coupling term yields

$$-\frac{1}{\sigma^2} \int_0^t \mu'(s) \bar{X}_s ds = -\frac{\mu(t)\ell - \mu(0)x_0}{\sigma^2} + \frac{\ell - x_0}{\sigma^2 t} \int_0^t \mu(s) ds. \quad (6)$$

A key structural consequence emerges upon substitution: the boundary potential term cancels exactly. Defining the *cumulative mean displacement*  $M(t) := \int_0^t \mu(s) ds$ , and completing the square with the intrinsic energy contribution, the exponential argument of the FHT density reduces to the remarkably simple form

$$-\frac{(\ell - x_0 - M(t))^2}{2\sigma^2 t}. \quad (7)$$

This result reveals a fundamental insight: time-varying drift influences arrival statistics primarily through a deterministic displacement of the effective boundary distance. The FHT density thus retains an IG-type exponential structure (see [20, Appendix A]), with the classical constant-drift distance replaced by a time-dependent cumulative displacement.

While this exponential core determines the macroscopic timing of arrivals, the amplitude prefactor arises from boundary-crossing dynamics, which we address next.

### III. INSTANTANEOUS FLUX MODULATION AND EXPECTED POSITIVE FLUX

While the exponential core in (7) captures timing shifts through the cumulative displacement  $M(t)$ , the instantaneous amplitude depends on stochastic boundary-crossing dynamics. Deterministic flux approximations break down under strong

backflow ( $\mu(t) < 0$ ), producing artificial truncation despite diffusion-driven arrivals. We therefore introduce the diffusion-consistent Expected Positive Flux (EPF) formulation.

#### A. Diffusion-Scaled Flux

First, we define the diffusion-scaled mean flux factor  $F_{\text{mean}}(t)$ . Instead of allowing the instantaneous velocity fluctuation  $(\mu(t) - v_0)$  to scale linearly with time—which leads to severe overestimation (overshoot) of late-arriving peaks—we strictly constrain its impact by the characteristic diffusion length  $\sqrt{\sigma^2 t}$ ,

$$F_{\text{mean}}(t) = \ell + (\mu(t) - v_0) \sqrt{\sigma^2 t}. \quad (8)$$

Physically, this scaling reflects the fact that as the particle cloud disperses over time, its spatial concentration near the boundary decreases. Consequently, a given velocity fluctuation should push a progressively smaller fraction of the ensemble across the boundary compared to the initial, highly concentrated stage. By tying the drift impact to the diffusion-induced standard deviation, this structural scaling ensures that the flux perturbation correctly mirrors the actual spatial dispersion of the Brownian particles over time.

#### B. Expected Positive Flux Formulation

To prevent non-physical truncation during backflow phases, we model the instantaneous boundary flux as a Gaussian random variable, where the macroscopic flux  $F_{\text{mean}}(t)$  serves as the mean and the local diffusion scale  $S(t) = \sqrt{\sigma^2 t}$  as the standard deviation. This Gaussian approximation follows from the local central-limit scaling of diffusive fluctuations near the boundary.

The effective arrival rate is governed by the expectation of the strictly positive components of this flux distribution. By defining the standardized flux state  $Z(t) = F_{\text{mean}}(t)/S(t)$ , the smooth EPF  $F_{\text{smooth}}(t)$  is derived as

$$F_{\text{smooth}}(t) = F_{\text{mean}}(t) \Phi(Z(t)) + S(t) \phi(Z(t)), \quad (9)$$

where  $\Phi(\cdot)$  and  $\phi(\cdot)$  are the CDF and PDF of the standard normal distribution, respectively.

The EPF operator in (9) acts as a rigorous, physics-informed “soft-plus” function, effectively serving as a non-linear rectification mechanism for the boundary flux. During forward flow stages ( $Z \gg 0$ ),  $F_{\text{smooth}} \approx F_{\text{mean}}$ , perfectly preserving the heightened peak arrivals. Conversely, during severe backflow ( $Z < 0$ ), the EPF yields a smooth, strictly positive tail driven purely by the diffusion term  $S(t)\phi(Z)$ , accurately preventing the density from collapsing to zero.

#### C. The Corrected-Inverse-Gaussian Channel Model

The preceding analysis reveals that the FHT density under time-varying drift admits a natural two-layer structure. The exponential component is governed by the cumulative displacement  $M(t)$ , which captures the macroscopic *timing shift* induced by nonstationary drift. The *amplitude prefactor*, in contrast, is determined by stochastic boundary-crossing dynamics and must account for diffusion-driven flux fluctuations.

By combining the exponential core derived in (7) with EPF formulation in (9), we obtain a closed-form (approximated) analytical characterization of the FHT density under time-varying drift.

**Main Result (Corrected-Inverse-Gaussian Density).** *Under deterministic time-varying drift  $\mu(t)$  and diffusion coefficient  $\sigma^2$ , the FHT density at an absorbing boundary  $\ell$  is approximated by the C-IG formula,*

$$f_{C-IG}(t) = \frac{F_{\text{smooth}}(t)}{\sqrt{2\pi\sigma^2 t^3}} \exp\left(-\frac{(\ell - x_0 - M(t))^2}{2\sigma^2 t}\right). \quad (10)$$

**Remark (Computational Complexity and Receiver Design).** A key advantage of the proposed C-IG density is its  $\mathcal{O}(1)$  evaluation complexity per time instance, requiring only basic algebraic and standard normal distribution evaluations. In contrast, obtaining the exact FHT density under nonstationary drift typically requires either high-latency Monte Carlo path simulations or recursive numerical integration of Volterra-type equations [15], both of which entail significant computational overhead that scales with the desired precision. By providing a tractable  $\mathcal{O}(1)$  likelihood function, the C-IG model bypasses these numerical bottlenecks, making advanced signal processing techniques, such as real-time Maximum Likelihood (ML) detection and dynamic channel equalization, practically feasible for nonstationary MC receivers.

This expression retains the classical IG exponential structure while incorporating two essential corrections: a time-dependent effective displacement that captures drift-induced phase shifts, and a diffusion-consistent stochastic flux modulation that ensures physically realistic behavior under strong backflow conditions.

#### IV. NUMERICAL RESULTS

We validate the C-IG model via particle-level Monte Carlo simulations implemented in MATLAB (with random seed 42) using  $N = 10^5$  trajectories and a fixed time-step  $\Delta t = 10^{-3}$ . To ensure sub-step precision, arrival times are resolved via linear interpolation at the boundary. Unless otherwise specified, we set the baseline drift  $v_0 = 1.0$ , diffusion coefficient  $\sigma^2 = 2.0$ , and boundary distance  $\ell = 5.0$  in dimensionless units.

##### A. Validation Under Strongly Pulsatile Drift

We first consider a sinusoidal drift profile  $\mu(t) = v_0 + A \sin(\omega t)$ , with an angular frequency  $\omega = 2\pi$ . Drift magnitude is normalized relative to the diffusion scale, as is standard in molecular communication studies [1]. To emphasize nonstationary effects, we adopt an amplitude ratio  $A/v_0 = 2$  (i.e.,  $A = 2.0$ ), representing a strongly pulsatile regime with periodic flow reversal, consistent with physiological transport scenarios [6], [7].

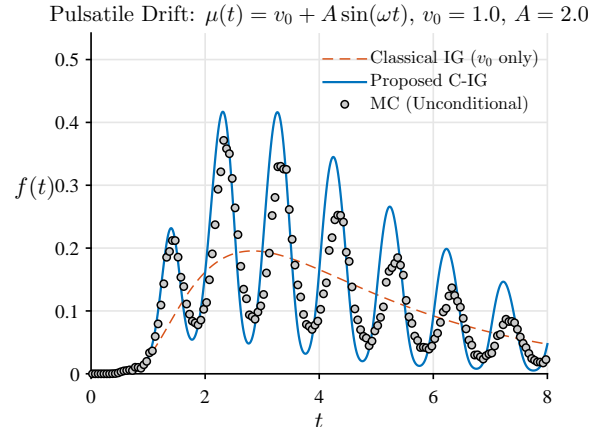


Fig. 3. First-hitting-time distributions under sinusoidal pulsatile drift. The proposed C-IG density captures phase shifts (which complicate timing synchronization) and amplitude modulation (which exacerbates ISI), whereas the classical IG model fails to represent nonstationary transport effects.

Fig. 3 compares the FHT distributions. The classical IG model, which assumes constant drift  $v_0$ , fails to capture the oscillatory modulation of arrival density—a phenomenon that induces severe non-traditional inter-symbol interference (ISI)—and substantially overestimates peak amplitudes. In contrast, the proposed C-IG density closely matches the Monte Carlo results across all time regimes. The cumulative displacement  $M(t)$  accurately predicts phase-shifted arrival peaks, which are critical sources of timing synchronization errors, while the EPF mechanism preserves nonzero arrival probability during transient backflow intervals.

These results demonstrate that the C-IG framework extends the analytical tractability of the IG structure to strongly time-varying drift conditions, while retaining constant-complexity evaluation, making it highly suitable for signal processing applications at the receiver.

##### B. Robustness Under Abrupt Drift Switching

To verify that the model is not tuned exclusively to sinusoidal profiles, we next consider a single-step switching drift:

$$\mu(t) = \begin{cases} v_0 + A, & t < T_{sw}, \\ v_0 - A, & t \geq T_{sw}, \end{cases} \quad (11)$$

where the switching time is set to  $T_{sw} = 1.5$ . This models a sudden flow reversal (e.g., microfluidic pullback clearing) with a 50% duty cycle so that the average velocity matches the classical IG baseline.

This profile introduces a discontinuous drift derivative and large total variation in the driving field, under which the classical IG model exhibits severe peak misalignment and amplitude distortion, leading to severely suboptimal detection if directly applied to receiver design. In contrast, the C-IG density remains stable: the cumulative displacement  $M(t)$  captures the macroscopic phase transition at the switching time, while the EPF prefactor prevents artificial truncation, accurately reproducing both sharp peak formation and post-switch depletion observed in Monte Carlo simulations (Fig. 4).

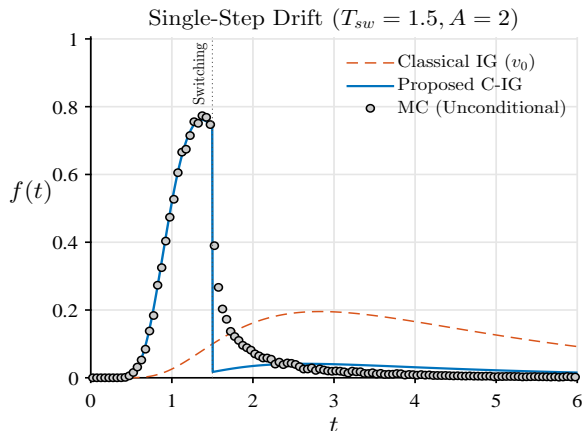


Fig. 4. First-hitting-time distributions under single-step drift switching with  $T_{sw} = 1.5$ . The proposed C-IG density remains accurate under abrupt drift variation, while the classical IG model fails to align with the observed phase transition, highlighting its inadequacy for reliable symbol synchronization.

**Remark (On Prefactor Stabilization).** For highly discontinuous drift profiles such as abrupt switching, we adopt a running-average baseline  $\bar{\mu}(t) = M(t)/t$  in the EPF prefactor to avoid overshoot induced by large instantaneous drift deviations. For smooth periodic profiles, the instantaneous formulation  $\mu(t) - v_0$  is sufficient and yields nearly identical results. This refinement improves numerical stability under large total-variation drift without altering the exponential core structure of the C-IG model.

### C. Model Limitations and Practical Implications

While the C-IG model exhibits strong agreement with Monte Carlo simulations, minor deviations appear in later arrival peaks under highly nonstationary drift. These discrepancies arise from irreversible absorption effects—higher-order memory phenomena where early-arriving particles are permanently removed, gradually skewing the surviving population in a manner not captured by the closed-form density. Nevertheless, these deviations remain secondary compared to the substantial mismatch of the stationary IG baseline (see Fig. 3). By accurately capturing phase modulation and amplitude restructuring while preserving constant-complexity evaluation, the C-IG framework remains well-suited for system-level analysis, receiver optimization, and real-time channel estimation in nonstationary MC systems.

## V. CONCLUSION

This paper established a tractable analytical framework for modeling FHT dynamics under nonstationary drift. By leveraging a change-of-measure perspective, we derived the C-IG density (10)—a closed-form expression with  $\mathcal{O}(1)$  evaluation complexity that generalizes the classical IG model to dynamic environments. Particle-level simulations confirmed that the C-IG model accurately captures complex transport phenomena, including phase modulation, multi-pulse dispersion, and transient backflow, while bypassing the latency bottlenecks of traditional numerical solvers. This framework bridges the gap between physics-faithful transport modeling and tractable

channel analysis, providing a robust foundation for the signal processing design and optimization of nonstationary biological and MC receivers.

## ACKNOWLEDGMENT

This work was supported by the National Science and Technology Council of Taiwan (NSTC 113-2115-M-008-013-MY3).

## REFERENCES

- [1] V. Jamali, A. Ahmadzadeh, W. Wicke, A. Noel, and R. Schober, "Channel modeling for diffusive molecular communication—a tutorial review," *Proc. IEEE*, vol. 107, no. 7, pp. 1256–1301, 2019.
- [2] N. Farsad, H. B. Yilmaz, A. Eckford, C.-B. Chae, and W. Guo, "A comprehensive survey of recent advancements in molecular communication," *IEEE Commun. Surveys Tuts.*, vol. 18, no. 3, pp. 1887–1919, 2016.
- [3] M. Pierobon and I. F. Akyildiz, "A physical end-to-end model for molecular communication in nanonetworks," *IEEE J. Sel. Areas Commun.*, vol. 28, no. 4, pp. 602–611, 2010.
- [4] A. Fick, "On liquid diffusion," *Philos. Mag.*, vol. 10, no. 63, pp. 30–39, 1855.
- [5] K. V. Srinivas, A. W. Eckford, and R. S. Adve, "Molecular communication in fluid media: The additive inverse Gaussian noise channel," *IEEE Trans. Inf. Theory*, vol. 58, no. 7, pp. 4678–4692, 2012.
- [6] Y. Chahibi, I. F. Akyildiz, S. Balasubramaniam, and Y. Koucheryavy, "Molecular communication modeling of antibody-mediated drug delivery systems," *IEEE Trans. Biomed. Eng.*, vol. 62, no. 7, pp. 1683–1695, 2015.
- [7] L. C. Wille, C. Pfannenmüller, and J. Kirchner, "From steady to pulsatile flow in molecular communication: Propagation of nanoparticles in mid-sized arteries," *IEEE Trans. Mol. Biol. Multi-Scale Commun.*, 2025.
- [8] S. Cho, T. C. Sykes, J. P. Coon, and A. A. Castrojo-Pita, "Electrophoretic molecular communication with time-varying electric fields," *Nano Commun. Netw.*, vol. 31, p. 100381, 2022.
- [9] P.-C. Chou, Y.-F. Lo, C.-H. Lee, and P.-C. Yeh, "Molecular communications enhanced by time-varying electric field," *IEEE Trans. Nanobiosci.*, vol. 21, no. 2, pp. 301–311, 2022.
- [10] S. Uchida, "The pulsating viscous flow superposed on the steady laminar motion of incompressible fluid in a circular pipe," *Z. Angew. Math. Phys.*, vol. 7, no. 5, pp. 403–422, 1956.
- [11] T. Koike-Akino, J. Suzuki, and P. V. Orlik, "Molecular signaling design exploiting cyclostationary drift-diffusion fluid," in *Proc. IEEE Global Commun. Conf. (GLOBECOM)*, Singapore, Dec. 2017.
- [12] T. N. Cao, A. Ahmadzadeh, V. Jamali, W. Wicke, P. L. Yeoh, J. Evans, and R. Schober, "Diffusive mobile MC with absorbing receivers: Stochastic analysis and applications," *IEEE Trans. Mol. Biol. Multi-Scale Commun.*, vol. 5, no. 2, pp. 84–99, 2020.
- [13] B.-H. Koo, C. Lee, H. B. Yilmaz, N. Farsad, A. W. Eckford, and C.-B. Chae, "Molecular MIMO: From theory to prototype," *IEEE J. Sel. Areas Commun.*, vol. 34, no. 3, pp. 600–614, 2016.
- [14] D. Arifler and D. Arifler, "Monte carlo analysis of molecule absorption probabilities in diffusion-based nanoscale communication systems with multiple receivers," *IEEE Trans. Nanobiosci.*, vol. 16, no. 3, pp. 157–165, 2017.
- [15] J. Durbin, "The first-passage density of a continuous gaussian process to a general boundary," *J. Appl. Probab.*, vol. 22, no. 1, pp. 99–122, 1985.
- [16] S. Redner, *A Guide to First-Passage Processes*. Cambridge Univ. Press, 2001.
- [17] B. Øksendal, *Stochastic Differential Equations: An Introduction with Applications*, 6th ed. Springer, 2002.
- [18] O. Calin, *An Informal Introduction to Stochastic Calculus with Applications*. World Scientific, 2015.
- [19] D. Dürr and A. Bach, "The onsager-machlup function as lagrangian for the most probable path of a diffusion process," *Commun. Math. Phys.*, vol. 60, no. 2, pp. 153–170, 1978.
- [20] Y.-C. Lee, P.-C. Yeh, and C.-H. Lee, "Exact 3-D channel impulse response under uniform drift for absorbing spherical receivers," *IEEE Commun. Lett.*, vol. 30, pp. 1290–1294, 2026.